Forgács T, Sarhosis V, Bagi K.

Influence of construction method on the load bearing capacity of skew masonry arches.

***Engineering Structures* 2018, 168(1), 612–627.**

Influence of construction method on the load bearing capacity of skew masonry arches

Tamás FORGÁCS[a], Vasilis SARHOSIS[b], Katalin BAGI[a]

[a] *Dept. of Structural Mechanics, Budapest University of Technology and Economics,*
forgacs.tamas@epito.bme.hu; kbagi@mail.bme.hu
[b]*School of ~~Civil~~ Engineering ~~and Geosciences~~, Newcastle University, Newcastle Upon Tyne, NE1 7RU, UK,*
Vasilis.Sarhosis@newcastle.ac.uk

Formatted: Font: Not Italic

Abstract

This paper investigates the influence of construction method (e.g. false skew, helicoidal and logarithmic method) on the mechanical behaviour and load carrying capacity of single span skew masonry arches. Simulations were performed with the three dimensional computational software ~~3DEC~~, based on the Discrete Element Method of analysis. ~~Within 3DEC, e~~Each stone/brick of the masonry skew arch was represented by a distinct block. Mortar joints were modelled as zero thickness interfaces which can open and close depending on the magnitude and direction of the stresses applied to them. The variables investigated were the construction method, the angle of skew, the size of masonry blocks and the critical location of the live load along the span of the arch. At each skew arch, a full width vertical line load was applied incrementally until collapse. From the results analysis, it was found that for a skew masonry arch constructed using the false skew method, as the angle of skew increase, sliding between voussoirs in the arch increases and failure load decreases. However, for skew masonry arches constructed using the helicoidal and logarithmic method, as the angle of skew increases, the failure load increases. Three different characteristic failure modes were identified depending on the contact friction angle and the method of construction. These observations provide new insight into the behaviour and lead to suggestions for understanding the load carrying capacity and failure mode of skew arches.

Keywords: *Masonry, arch, discrete element method, numerical modelling, cracking, in-plane loading.*

Notation list

Ω	angle of skew
R	mid-radius of the arch barrel
s	span of the arch
b	breadt of the arch (parallel to the abutments)
t	barrel thickness
L	length of the voussoir
W	width of the voussoir
x	loading position (measured from the abutments)
k_n	contact elastic normal stiffness
k_s	contact elastic shear stiffness
φ	internal friction of contact
φ_{res}	residual internal friction of contact
c	cohesion of contact
c_{res}	residual cohesion of contact
f_t	tensile strength of the contact
ψ	dilatation angle of contact
ρ	density of the blocks
σ	normal stress
τ	shear stress

1. Introduction

Masonry arch bridges have been used for at least four millennia. In Europe alone, there are thousands of masonry arch bridges which still form part of the highway and railway networks. As a result of the over-conservative design methods used for their construction in the past, these bridges are usually able to carry the even-increasing live loads from modern day traffic. Also, masonry arch bridges have been proved to be an extremely durable structural form and considered to be aesthetically pleasing. However, most of these bridges are now old and are deteriorating over time [1]~~(Brencich and Morbiducci 2007)~~. Moreover, the different materials and methods of construction (e.g. masonry skew arches which enable to span obstacles at an angle) used in these bridges will influence their strength and stiffness [2, 3]~~(Sarhosis et al. 2016b; Forgács et al. 2017)~~.

Over the last two decades, considerable effort has been put into gaining a greater understanding of the behaviour of masonry arch bridges with a view to improve resilience of transport corridors and efficiency when assessing the serviceability and ultimate limit state behaviour of such bridges [2] ~~(Sarhosis et al. 2016b)~~. However, many approaches (e.g. analytical methods and numerical techniques) used for the assessment of masonry arches has been recognised as being highly conservative and predict collapse loads far lower than predicted by experience [2]~~(Sarhosis et al. 2016b)~~. Furthermore, although it is well understood that masonry arch bridges behave in a three dimensional manner [3-5]~~(Hodgson 1996; Wang 2004; Forgács et al. 2017),~~ a great deal of work has been carried out to assess the strength of square span masonry arch bridges using mainly two dimensional methods of analysis [6-9]~~(Heyman 1966; Gilbert 1993; Page 1993; Melbourne and Hodgson 1995)~~. For example, in UK as well as other parts of Europe, the most commonly used method for the assessment of masonry arch bridges in the industry is the "MEXE". This is a semi-empirical approach based on an elastic analysis by Pippard et al. [10]~~(1936)~~ who modelled the arch barrel as linear elastic, segmental in shape, pinned at its support and carrying a central point load. Although the approach is quick and easy to use, it has been found to be over-conservative and in some cases highly subjective to parameters used for the estimation of the maximum load. Other approaches used by the industry ~~in UK~~ are mostly based on 2D limit analysis. Using the robustness of linear programming ultimate load bearing capacity and the failure mode can be estimated.~~a) The static theorem of plastic limit analysis (developed into the Archie-M software) which uses simple equilibrium calculations (the self-weigh of the arch barrel and live loads are balanced by forces between the blocks); and b) the RING software which uses the kinematic theorem of limit analysis to identify the collapse state with the smallest external loading and hence predict the ultimate load.~~

Commented [T1]: This are techniques based on plastic limit analysis. The problem is solved with linear programming. Which means, that they maximize the live load such that the equilibrium equations and the linear inequalities (hinging and sliding constraints) are satisfied. Considering the duality theorem of linear programming, the optimal solution of the primal problem will be equal with the solution of the dual problem. So there is no such that: this software works according to the static theorem and the other works according to the kinematic theorem…

With the use of sophisticated methods of analysis like Finite Element Method (FEM), efforts have been made to understand the three dimensional behaviour of arches (e.g. [11-14]~~Fanning and Boothby 2001; Zhang et al 2016; Milani and Lourenço 2012~~). The disadvantages of the finite element method are mainly associated with: a) relatively high computational cost in comparison to limit analysis; b) crack

development cannot be obtained without ~~an a~~ a priori knowledge of where to expect cracks; and c) convergence difficulties if blocks fall or slide excessively. An alternative and appealing approach is represented by the Distinct Element Method (DEM), where the discrete nature of the masonry arch is truly incorporated [15]~~(Sarhosis et al. 2016a)~~. The advantage of the DEM is that it considers the arch as a collection of separate voussoirs able to move and rotate relative to each other; the main disadvantage is the often huge computational cost, even if compared to FEM [16]~~(Giamundo et al. 2014)~~. The DEM was initially developed by Cundall ([17])~~(1971)~~ to model blocky-rock systems and sliding of individual pieces of stones along joints. The approach was later used to model masonry structures including arches ([3, 18, 19, 29, 30])~~(Lemos 2007; Sarhosis et al. 2014a; Forgács et al. 2017)~~, where failure occurs along mortar joints. These studies demonstrated that DEM is a suitable method to perform analysis of masonry arches and to describe realistically the ultimate load and failure mechanism.

Skew arches, i.e. arches that span obstacles not perpendicularly but at an angle, are most common in areas rich in rivulets or valleys of varying directions, e.g. around delta firths. During the industrial revolution the number of skew arches started to increase rapidly, since the straightness of the railway track was one of the most important aspect in the course of the design. Three main techniques were suggested for their construction in the 19th Century: (1) the false skew arch; (2) the helicoidal method; and (3) the logarithmic method (see their description below in Section 3, or in more detail in Forgács et al. [3] ~~(2017)~~). **Figure** 1 shows stone masonry skew arch bridges constructed using different construction methods~~techniques~~.

(a) False skew arch: Maxwell Creek Bridge, Napa County, California, USA ~~Photo:~~(*courtesy of Mark Yashinsky*)

Formatted: Font: Italic

(b) Helicoidal method [19]

(c) Logarithmic method: LLC-74A bridge, Adlington, UK

~~*Photo:*~~ *(courtesy of ~~-~~Peter Robinson)*

Figure 1. Skew arch bridges constructed by different techniques

Over the last 30 years, although significant research work has been carried out to understand the mechanical behaviour of arches, limited research been carried out to understand the mechanical behaviour of skew arches. ~~There are only a few experimental tests regarding skew masonry arches.~~ Abdunur ~~(~~[20]~~)~~ investigated a shallow, 45° helicoidal brickwork skew arch consisting of two rings ~~of bricks~~. The arch was loaded to collapse with a line load parallel to the abutments. ~~In the tests of~~Later, Wang ~~(~~[5]~~)~~ tested a similar, but a more narrow ~~structure~~ skew arch~~was~~ subjected to a ~~loaded with a~~ patch load at quarter span. The arch failed due to the formation of hinged mechanism. The hinges were parallel to the abutments, and this was mainly due to the stiffening effect of internal spandrel walls and masonry backing. In addition, Hendry et al. ~~(~~[21]~~)~~ and Melbourne ~~(~~[9]~~)~~ investigated a 16 degrees skewed semi-circular arch masonry bridge~~s, where~~ with backfill and spandrel walls ~~were present~~. Failure was due to a compressive failure of the arch beneath the loading position. Moreover, Sarhosis et al. [19] investigated numerically the influence of skew angle on segmental and circular skew arches constructed with joint parallel to springing. The behaviour of skew arches compared against those of

Commented [VS2]: We can cite here my first paper on skew arches….

Formatted: Font: Italic

Formatted: Font: Italic

"square" or regular arches. It was found that an increase in the angle of skew will increase the twisting behaviour of the arch and will cause failure to occur at a lower load. Also, the effect of angle of skew on the ultimate load is more significant for segmental rather than circular arches.

The aim of this paper is ~~now~~ to extend ~~and continue~~ the previous study carried out by the authors [3] and investigate the influence of construction method on the load carrying capacity of skew masonry arches. It is anticipated that such results will provide useful information and guidance to design engineers and practitioners. Using the three-dimensional DEM software ~~3DEC (Itasca 2004~~[22]~~)~~, computational models were developed to predict the ultimate behaviour of different in construction masonry skew arches with different skew angles. DEM is well suited for collapse analysis of stone masonry structures since: a) large displacements and rotations between blocks, including their partial or complete detachment, can be simulated; b) contacts between blocks are automatically detected and updated as block motion occurs; and c) progressive failure associated with crack propagation can be simulated.

At the present study, the false skew, the logarithmic, and the helicoidal method of construction of skew arches have been studied. According to [1, 23] the rise-to-span ratio of masonry bridge stock varies significantly from country to country ~~in a wide range~~. ~~The~~ However, from [1, 23] it was found that the most common shape ~~was~~ for skew masonry arches is that of ~~the~~a semi-circular (e.g. 50% of masonry bridges on Italian railways, 92% of Hungarian masonry bridges). Therefore, as part of this study, semi-circular arches (with rise-to-span ratio: 1:2) were investigated ~~in this work only~~. In addition, ~~S~~since the intention of the authors was to investigate the effect of the arch barrel geometry, neither the fill nor the spandrels or parapets have been studied herein~~included at this stage~~. The variables investigated were the construction method, the angle of skew, the size of masonry blocks and the critical location along the span of the arch where smallest load can be carried.

Section 2 gives a short overview of the applied numerical modelling techniques. Geometrical and material characteristics of the arches studied will be introduced in detail in Section 3. Section 4 presents the simulation results in detail. Finally, Section 5 draws the most important conclusions.

2. The applied discrete element software for modelling masonry arches

The software applied in the present study~~, 3DEC (a commercial code released by Itasca)~~ is based on the discrete element method and is able to represent masonry structures as a set of polyhedral blocks [15]~~(Sarhosis et al. 2016a)~~. Mortar joints are represented as interfaces/surfaces where mechanical interaction between blocks takes place. This interaction is governed by appropriate constitutive laws ~~(Sarhosis et al. 2015)~~. The motion of the blocks is simulated throughout a series of small but finite time-

steps, using the central difference technique to numerically integrate the Newtonian equations of motion.

2.1 Representation of masonry units

In ~~3DEC~~DEM model developed, the blocks may be convex or concave in shape and can be rigid or deformable. In the present study blocks were assumed to behave as rigid bodies. Each block had six degrees of freedom (three translational and three rotational). ~~The deformability of the blocks was represented by the material properties at the contacts [3, 24, 25](Simon and Bagi 2016, Forgács et al 2017; Sarhosis et al. 2014b).~~

2.2 Recognition and geometrical representation of joints between masonry units

The DEM software automatically keeps track of the contact topology. Contact means that a point of a block penetrates into another, neighbouring block. The contact detection algorithm recognizes these situations, and provides a unit normal vector, which defines the plane along which sliding can occur. This unit normal changes its direction continuously as the two blocks move relative to ~~one~~ each other~~another~~. Similarly to some other DEM codes which use ~~with~~ polyhedral elements (e.g. in certain versions of the Non-Smooth Contact Dynamics method), 3DEC applies the "common plane method" ~~(~~[3, 22]~~, 2004; Forgács et al, 2017)~~.

The "*common plane*" is defined as the solution of the optimization problem "*Maximize the gap between the common plane and the closest vertex"* or, equivalently, "*Minimize the overlap between the common-plane and the vertex with the greatest overlap*". Contact exists if the overlap is positive, i.e., if the gap is negative between the two blocks. The normal vector of the common plane is used as the contact normal. Details are not presented here for simplicity: the interested reader is advised to consult ~~the Itasca (2004) manual~~to refer to [22].

The basis of the mechanical calculations is the relative velocity of the suitably chosen pairs of material points on the two touching faces. The normal and tangential components of the increment of relative translation vector belonging to such a pair is multiplied with the actual normal and shear stiffness of the contact, in order to define the increments of uniformly distributed normal and shear forces belonging to the neighbourhood of the pair.

2.3 Constitutive models for contacts

The mechanical behaviour of contacts is modelled with the help of contact stiffness defined in the normal and shear directions, relating distributed normal and tangential contact forces to relative displacements (**Figure 2**). According to Lemos ~~(~~[18]~~2007)~~, the normal stiffness can have different

physical interpretations even in those cases when the blocks are deformable: (a) in the case of mortared joints, the normal stiffness can be directly related to mortar thickness and its mechanical properties ~~(Sarhosis et al. 2015)~~; (b) For dry joints, rough and irregular contact surfaces have a finite stiffness against penetration, which is reflected by the contact normal stiffness. In the shear direction, shear stiffness plays a similar role and Coulomb friction sets a limit to the sub-contact shear stress magnitude. ~~In case of perfectly rigid blocks in the 3DEC, on the other hand, the contact stiffness data have to represent the block deformability as well; [24]Simon and Bagi (2016) provide a short analysis how to relate the contact stiffness parameters to the mechanical data of the contacting voussoirs.~~

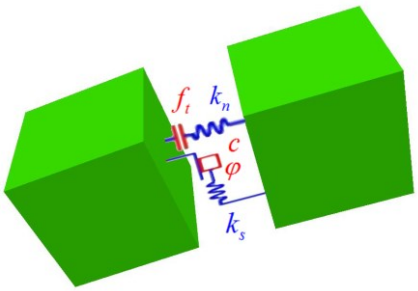

(a)

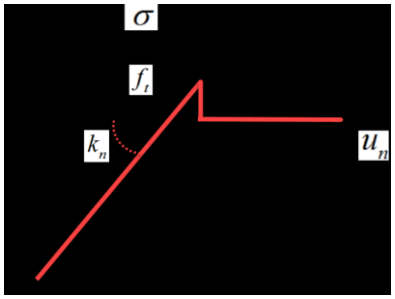

(b)

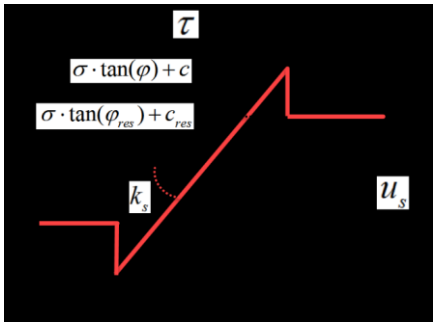

(c)

Figure 2. Contact constitutive law implemented in this study (a) mechanical representation of contacts; (b) normal stress against normal displacement relationship; (c) shear stress against shear displacement relationship

Considering the degradation and material deterioration in masonry arch bridges, we could assume that the tensile and cohesive strength of mortar is very small and relatively zero. Although, this assumption

is conservative, it could be adopted since this will provide the worst case scenario. In addition, assumptions related to the zero tensile strength of mortar in historic and old and deteriorated masonry has been done by others [6]. ~~the typical age of skew arch bridges, the cohesion and the tensile strength between the voussoirs might have large uncertainty, that is why we assumed cohesionless material without tensile strength Joint dilatation angle could also be included, in the present study this value was set to zero. Moreover, in the lack of appreciate data, the frictional angle was not decreased after sliding.~~

2.4 Calculation procedure

In the discrete element method, ~~The~~ the calculation of the motion of the system is done through a series of small but finite time steps. At the beginning of a time step, the force-displ-acement law applied at the contacts provides forces acting on the elements in addition to external loads like gravity or damping force; in this way the differential equation of translational motion can be written as:

$$\ddot{\underline{x}}(t) + \alpha \dot{\underline{x}}(t) = \frac{\underline{F}(t)}{m} + \underline{g} \qquad (1)$$

Commented [VS3]: Equation does not show properly..

where $\ddot{\underline{x}}(t)$ and $\dot{\underline{x}}(t)$ are the acceleration and the velocity vector of the centroid of the block, respectively; $\underline{F}(t)$ is the sum of forces acting on the block (contact + applied external forces, except gravitational forces); m is the mass of the block; α is the viscous (mass-proportional) damping constant; and $\underline{g}$ is the gravity acceleration vector. Time integration of equations of motion is done with the central finite difference scheme (**Figure 3**):

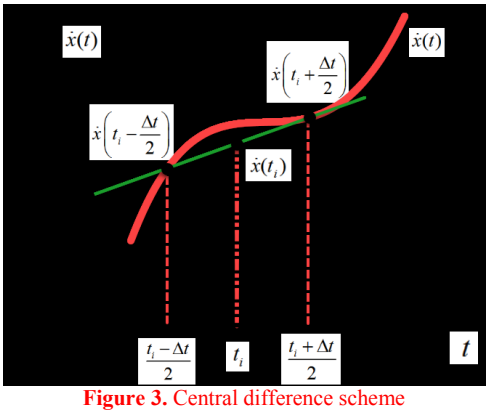

Figure 3. Central difference scheme

The translational velocities and the accelerations at time t can be approximated as:

$$\underline{\dot{x}}(t) = \frac{1}{2}\left[\underline{\dot{x}}\left(t-\frac{\Delta t}{2}\right)+\underline{\dot{x}}\left(t+\frac{\Delta t}{2}\right)\right] \tag{2}$$

$$\underline{\ddot{x}}(t) = \frac{1}{\Delta t}\left[\underline{\dot{x}}\left(t+\frac{\Delta t}{2}\right)-\underline{\dot{x}}\left(t-\frac{\Delta t}{2}\right)\right] \tag{3}$$

Inserting (2) and (3) into the differential equation of motion (1), the velocity at $(t+\Delta t/2)$ can be calculated as:

$$\underline{\dot{x}}\left(t+\frac{\Delta t}{2}\right) = \left[\left(1-\frac{\alpha\Delta t}{2}\right)\cdot\underline{\dot{x}}\left(t-\frac{\Delta t}{2}\right)+\left(\frac{\underline{F}(t)}{m}+\underline{g}\right)\cdot\Delta t\right]\cdot\frac{1}{1+\alpha\frac{\Delta t}{2}} \tag{4}$$

The rotational motion of the blocks can be calculated similarly. In this way, the motion of discrete elements can be followed. Since the time integration technique is explicit, convergence to static solutions can be received by means of different optional damping methods (see Forgács et al, ~~2017~~[3] for an overview).

3. Geometrical and mechanical characteristics of the analysed skew arches

A skew arch is a method of construction that enables masonry arch bridges to span obstacles at an angle. Bridges with a small amount of skew (i.e. less than 30º) were frequently constructed using bedding planes parallel to the abutments [9]~~(Melbourne and Hodgson, 1995)~~. However, bridges with large amount of skew present significant construction difficulties. **Figure ~~4~~ 3** shows the developed mid-surfaces of the three most prevalent methods of construction for a circular arch spanning at 45 degrees skew [8]~~(Page 1993)~~. **Figure ~~4a~~ 3a** shows the simplest form of construction ("false skew arch") where units are laid parallel to the abutments. **Figure ~~4b~~ 3b** shows the English or "helicoidal" method which is constructed such that the bed at the crown is perpendicular to the face of the arch. ~~to the longitudinal axis of the bridge.~~ For geometrical reasons and for the beds to remain parallel, the orientation of the block units causes the beds to "roll over" and thus rest on the springings at an angle. In this way, the coursing joints follow helix spirals. This is a relatively cheap method of construction since every voussoir is cut to the same shape. **Figure ~~4c~~ 3c** shows the French (or orthogonal or logarithmic) method which keeps the bed orthogonal with the local edge of the arch. This is the most expensive method of construction since it requires varying sized and shaped masonry blocks and needs availability of high skilled masons, since almost every block in the arch barrel is to be of different shape. The procedure used for the construction of such bridges and their mathematical curves are described in full detail by Rankine ~~(1867~~[26]~~)~~. The methodology used for the construction of the geometric models are presented at Forgács et al. ~~(2017~~[3]~~)~~

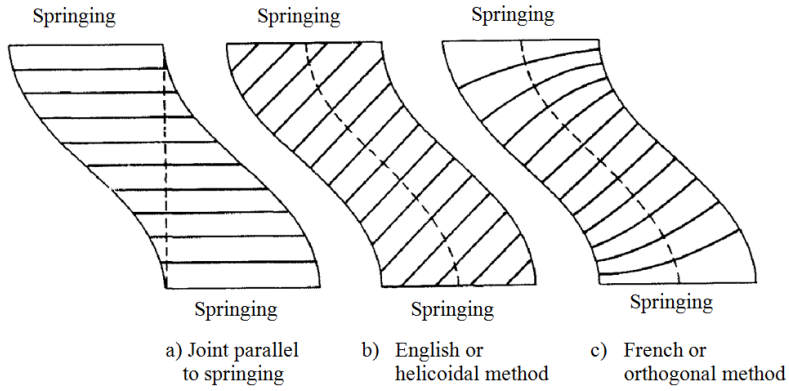

Figure ~~4~~3. Intrados of an arch spanning at 45^0 skew ~~(Page 1993~~[8]~~)~~

The characteristic geometrical parameters of a general skew arch are shown in **Figures ~~5~~ 4 and ~~6~~5.** The range of variation of geometrical characteristics for the arches used in the computational analysis is shown in **Table 1.** Geometric models representing skew masonry arches using different construction

methods are shown in **Figure 65**. Every investigated arch contained 41 courses of voussoirs counted along the arch. The stones ~~bricks~~ were arranged in a pattern where every second courses had a half-voussoir translation in the longitudinal direction. The arch barrels contained a single ring of stone voussoirs.

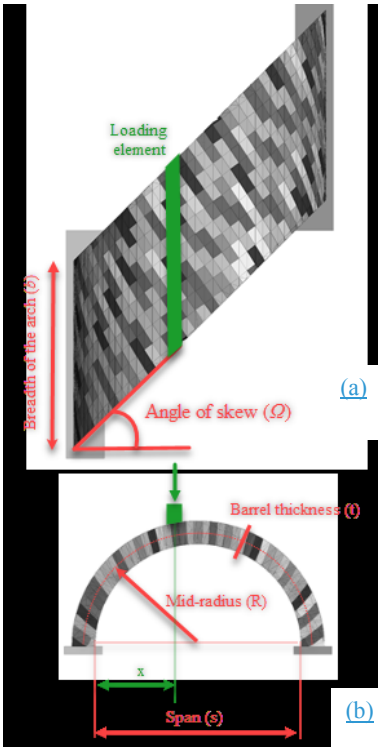

Figure ~~5~~ 4 – Geometrical parameters of skew arches: (a) plan view; (b) front view – note that the mortar joints were not oriented radially. This is the perspective plan view of a skew arch.

Table 1. Geometrical characteristics for the arches developed.

Mid-radius of the arch *R* [m]	Thickness of the arch, *t* *[m]*	Breadth of the arch *b* [m]	Angle of skew Ω [degrees]	Average length-to-width ratio of the voussoirs	Average block width *W* [m]
3.00	0.36; 0.60	5.00	0 to 45	2:1<*L*/*W*<3:1	~0.250

Formatted Table

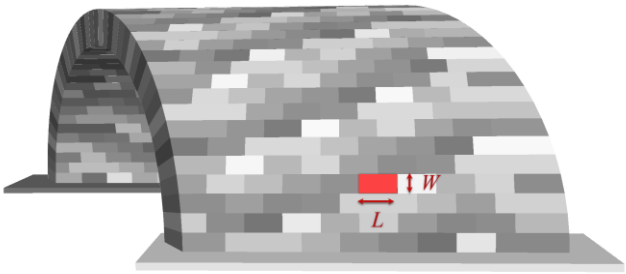

(a) False skew method

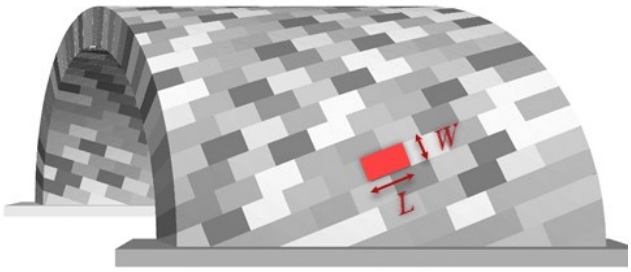

(b) Helicoidal method

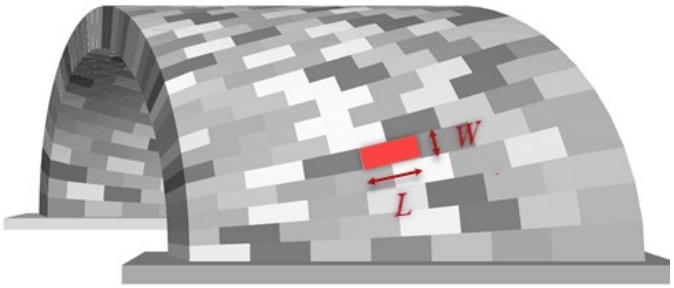

(c) Logarithmic method

Figure ~~6~~5. Typical geometry of 30° skew masonry arches constructed using a) false skew; b) helicoidal; c) logarithmic method

~~Since the intention of the authors was to investigate the effect of the arch geometry, the abutments of the arch were modelled as rigid supports in the vertical and horizontal directions.~~ ~~Depending~~ Since the intention of the authors was to investigate the effect of the arch geometry, the abutments of the arch were modelled as rigid supports in the vertical and horizontal directions. From Forgacs [3], depending

on the skewness of the arches the reaction force distribution at the abutments ~~is typically~~could be ~~-~~non-uniform. In the present study, s~~S~~ince the intention of the authors was to investigate the effect of the arch geometry, the abutments of the arch were modelled as rigid supports in the vertical and horizontal directions. Zhang et al. [2] investigated the influence of abutment stiffness on load bearing capacity in case of 45° skew arch, but there was no significant change in the behaviour. ~~Zhang et al. [2] investigated the influence of abutment stiffness on load bearing capacity in case of 45° skew arch, but there was no significant change in the behaviour.~~

Table 2. Properties of the joint interface for the development of the computational models

Joint Normal Stiffness ~~k_n~~ K_n [N/m^3]	Joint Shear Stiffness ~~k_s~~ K_s [N/m^3]	Joint Friction φ [degrees]	Joint Dilatation ψ [degrees]
7.64×10^9	1.79 ×10^9	20° to 50°	0°

Formatted Table

Formatted: Font: Not Italic

Self-weight effects were assigned as a gravitational load. Gravitational forces give rise to compressive forces within the blocks of the arch and result in the stabilisation of the arch. Every model was brought into equilibrium under its own self-weight, before applying any live load. During the numerical simulations, the external live load was applied on the extrados with the help of a loading element which was placed on the structure in parallel direction to the abutments of the arch (**Figure ~~5~~4**). The live load was applied as the gradual increase of the density of the loading element. Live load was increased sequentially in small load steps. The size of a load step was chosen in such a way that it was kept under the 1% of the expected ultimate load bearing capacity. At each load increment, the stability of the structure checked by ~~there was an attempt to equilibrate the structure. Two outcomes were possible: (a) the structure can be equilibrated: the model was considered to be in equilibrium when~~conforming that the maximum out-of-balance force ~~became~~ was less than 0.001% of the total weight of the structure~~; (b) the load increment cannot be equilibrated~~. ~~In the latter case, the out of balance force and the displacements of the structure started to increase rapidly.~~ The simulation was stopped when the maximum vertical displacement just below the application of the load in the structure exceeded 0.20 m; ~~such a large~~ such displacement suggested failure of the arch.

4. Validation of the numerical model

~~**Experimental comparison**~~

numerical model against those obtained from the experimental study presented in Wang [5]. In the laboratory, a shallow, skew masonry arch have been constructed and loaded to collapse with a patch load at quarter span ("Skew1" test). The arch had a rise-to span ratio equal to 1:4 and it was a 45° skew. The arch was constructed with standard size 220 mm × 102 mm × 73 mm Class A engineering bricks and composed of two rings. The joints were all nominally 10 mm thick with 1:2:9 (OPC : lime : sand) mortar. Bricks were arranged in header bond. In this way, no ring-separation allowed to occur. The load was applied at quarter span to the arch with the use of a hydraulic ram and was distributed through a timber plate with dimensions 150 mm × 150 mm which was embedded in mortar. During testing, the arch barrel was loaded to collapse without any prior loading. The average density of the brickwork was 2,240 kg/m^3. The experimental collapse load of the structure found to be equal to 16.27 kN. The cohesion, frictional angle and tensile strength of the mortar were not measured in the experiment. The geometry of the arch is show in **Figure 6**.

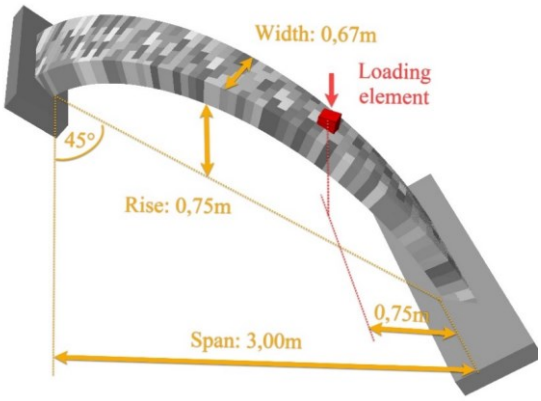

Figure 6. Experimental set up of the "Skew1" test Wang [5].

~~G~~A geometrical model representing the brickwork skew arch tested in the laboratory was created in the computational model. Bricks represented with rigid blocks separated by zero thickness interfaces to represent mortar. Since during the experiment no de-bonding between the two rings were allowed, in the computational model, the arch represented by a single ring. Material properties (e.g. frictional angle, cohesion and tensile strength etc.) used for the computational model were obtained from [12, 28] and shown in Table 3.

Table 3. Properties of the joint interface for the numerical-experimental comparison

Joint Normal Stiffness K_n [Pa/m]	Joint Shear Stiffness K_s [Pa/m]	Friction angle φ	Residual friction angle φ_{res}	Joint Dilatation ψ	Cohesive strength c [MPa]	Tensile strength f_t [MPa]
1.65×10^{10}	1.00×10^{10}	33°	33 °	0°	0.196	0.140

Commented [VS4]: please check this... why shear stiffness greater than normal stiffness???

Formatted: Font: 11 pt

Formatted: Font: 11 pt

Formatted: Font: 11 pt

Formatted: Font: 11 pt

A vertical velocity in the downward direction with magnitude 0.5 mm/s has been applied in the loading element until failure. A FISH sub-routine was written which was able to record reaction forces from the fixed velocity grid points acting on the spreader plate at each time-step. Also, histories of displacements just below the loading element were recorded at each time-step. The horizontal movement of the loading element was not constrained. A comparison of the experimental against the numerical failure modes is shown in **Figure 7**. From **Figure 7**, a good correlation was achieved between the numerical and experimental failure modes. Transverse cracking appeared at the abutments and at the ¾ and ¼ of the span of the arch.

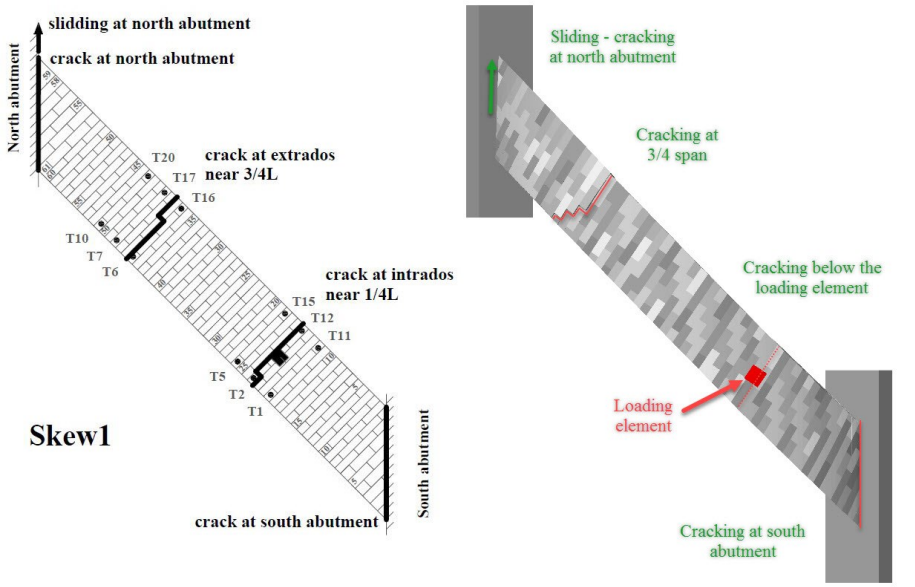

(a) (b)

Figure 7. Failure mechanisms in the experiment (a); and in the numerical model (b)

Figure 8a and Figure 8b represent the cracked and slipped surfaces of the arch at ultimate load. Three major cracks were observed and were located at: (i) the intrados below the loading element; (ii) at the extrados of the south abutment; and (iii) at the extrados at 3/4 span. Moreover a minor crack developed at the north abutment too. Excessive sliding was observed at the north abutment of the skew arch.

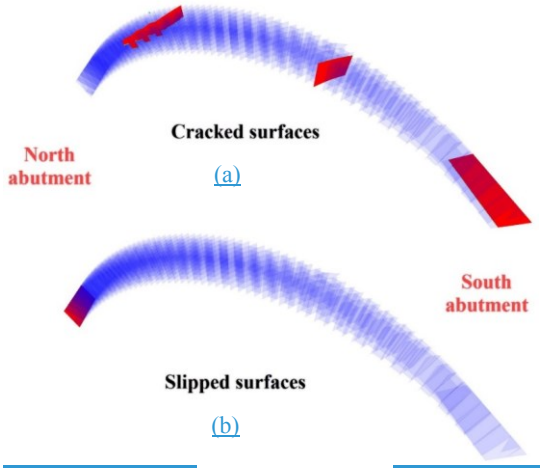

Figure 8. Joints cracked (a) and joints slipped (b) at ultimate load as obtained from the numerical model

Figure 9 compares the experimental and numerical load against displacement relationships. From the numerical simulation it was observed that the ultimate load bearing capacity of the skew arch depends strongly on the internal friction and cohesion between the masonry block elements. When the arch loaded at approximately 12 kN, the first cracks appeared at the south abutment and below the loading element. The north abutment started to slide at the ultimate load (~16 kN). After failure the load bearing capacity dropped with ~50%. Such findings coincide with the observations made in the experiment by Wang et al. [5].

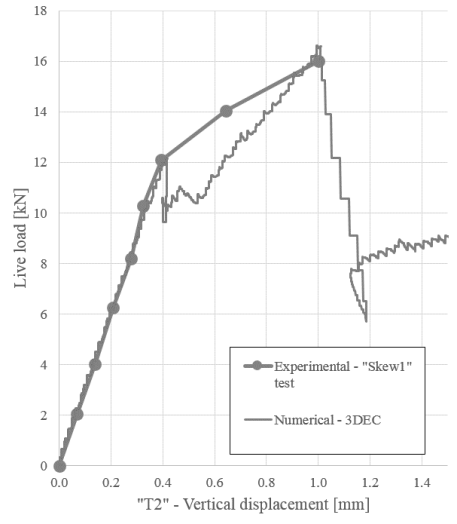

Figure 9. Comparison of experimental against numerical applied load against quarter span vertical displacements

~~4.~~5. Results and Discussion

A sensitivity study was undertaken to investigate the influence of different parameters and their interdependence on the load carrying capacity of masonry skew arches. In particular, the parameters investigated in this study are:

a) **Geometrical parameters:**
   - Construction method (false; helicoidal; logarithmic)
   - Element shape (L/W ratio)
   - Angle of skew
   - Barrel thickness (two values were applied: $0.12 \times R$ which is close to the minimum thickness of a regular arch; and $0.20 \times R$ which is a realistic value for skew masonry arches)

b) **Material parameters:**
   - Internal friction between the voussoirs in the arch

c) **Location of the externally applied load:**
   - Location of the externally applied load along the length of the arch

~~4~~5.1. Preliminary remarks: The effect of element shape and size

The length to width (L/W) ratio of masonry voussoirs in arches constructed using ~~the~~ different construction techniques can vary. While a false skew arch can be constructed using voussoirs of any L/W ratio, the complex geometry of arches constructed using the helicoidal and logarithmic ~~structures~~ restricts the shape of the voussoirs to be used for their construction. In a previous work of the authors (~~Forgács et al. 2017~~[3]), it was shown that the length to width ratio (L/W) of the individual voussoirs significantly influences the minimum necessary thickness of skew arches. Subsequently, in this study it was found that the shape of the voussoirs influences the load carrying capacity too. To quantify this hypothesis, a series of three dimensional computational models were developed on 45° skew arches having thickness (t) equal to $0.20 \times R$ and width of the voussoirs (W) equal to 0.25m. A fully distributed external load was also applied at x/s equal to 0.35 (i.e. near the third span) ~~(ref. to **Figure 6**)~~. Different L/W ratios were studied (i.e., W kept constant while L varied). The ultimate load bearing capacity was recorded and results are shown in **Figure ~~7~~10**.

From **Figure ~~7~~10,** the load bearing capacity of the logarithmic and helicoidal methods of construction show an almost linear dependence on the L/W ratio. However, the load bearing capacity of arches constructed using the false skew method in not proportional to the L/W ratio. Also, for arches constructed using the false skew method having voussoirs with length (L) greater than 1.5 times their width (W), the load bearing capacity is constant (i.e. does not depend on the length of the voussoirs)

and is equal to the load bearing capacity of the regular arch. In contrast, for voussoirs having *L*/*W* ratio equal to or below 1.5, the load bearing capacity significantly decreases as the length of the voussoirs (*L*) becomes smaller. This is due to the fact that the failure mode is also different from what observed for arches constructed with voussoirs having large *L*/*W* ratios (Ref. to Section 45.2.3 ~~and Figure 18~~).

Commented [T5]: we should not cite figure 18 here

Formatted: Highlight

In the numerical simulations that will be introduced in Section 4.2, the *L*/*W* ratio was intended to be kept around 3.0. Due to the geometrical restrictions for the construction of the different types of arches, the actual values had to vary from 2.5 to 3.1. This resulted in 5-6% ~~uncertainty~~ variation of the load bearing capacity. For the 30° skew arch constructed using the helicoidal method, the *L*/*W* ~~value~~ ratio was even lower and equal to 2.0. Th~~is is~~e load bearing capacity is thus 12% ~~smaller~~ lower ~~load bearing capacity~~ than what could have been obtained when the *L*/*W* ratio was equal to 3.0. In all simulations, t~~T~~he value of *W* was kept approximately the same ~~in all tests~~. Each arch was constructed with 41 blocks at the face of the arch. In this sense, no size effect ~~occured~~occurred.

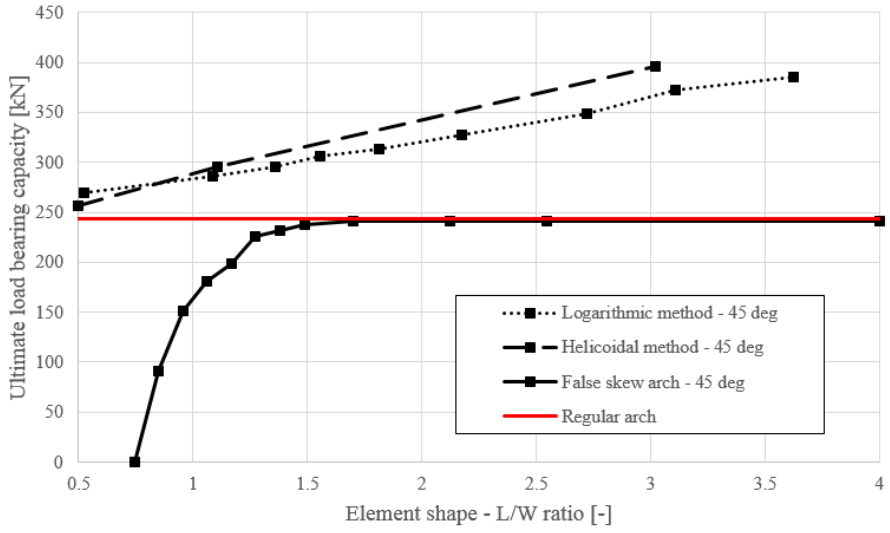

Figure ~~7~~10. Influence of element shape on the load bearing capacity of a 45° skew arch having barrel thickness equal to 0.20×*R*. Load applied at *x*/*s* = 0.35

~~4~~5.2 Interacting effect of the position of the externally applied load and of the contact friction angle

~~This Section shows how~~In this section, it is shown that the load bearing capacity of a skew arch ~~depends~~ varies with~~on~~ the position of the live load, and points out those situations when the magnitude of the contact friction may become important for the structural stability of the arch. ~~The aim of~~In Section

45.2.1 ~~is to point out that~~it is highlighted that even in the simplest case, i.e. straight arches with no sliding in the contact, the critical position of the load, depends on the arch thickness. Section 45.2.2 ~~will~~ analyses the case of skew arches in detail and appraise the effect of frictional resistance of the contacts. ~~The experiences~~Results obtained will then be explained in Section 45.2.3 where the failure mechanisms and the contact shear forces are visualized and discussed.

45.2.1 Inspiration: Application of external applied load on regular masonry arches

In order to assess the ultimate load carrying capacity of regular or "square" masonry arches, it is ~~a~~ common practice to apply the load at either ~~the~~ quarter, third or mid-span. An investigation has been carried out, using the commercial software LimitState: RING, to identify the critical loading position where the load carrying capacity of the arch is minimum. A regular, semi-circular arch (rise to span 1:2) was analysed having joints in the radial direction. The arch had a length equal to 3 m and a span equal to 5.64 m ~~**(Figure 4)**~~. The thickness of the arch varied from 0.120×*R* to 0.250×*R*. The joint friction angle was equal to 40° in all cases.

Figure ~~8~~ 11 shows the effect of the position of the application of the external load on the load carrying capacity of arches having different barrel thickness. When the thickness of the barrel is close to the critical thickness (i.e. 0.12×*R*), the critical position of the live load is at the mid-span. Increasing the barrel thickness, the critical position for live load gets shifted towards the support, to one-third and then nearly to quarter span, and the dependence of the critical load magnitude on its position becomes more expressed. Similar results were also obtained using ~~3DEC~~ numerical software.

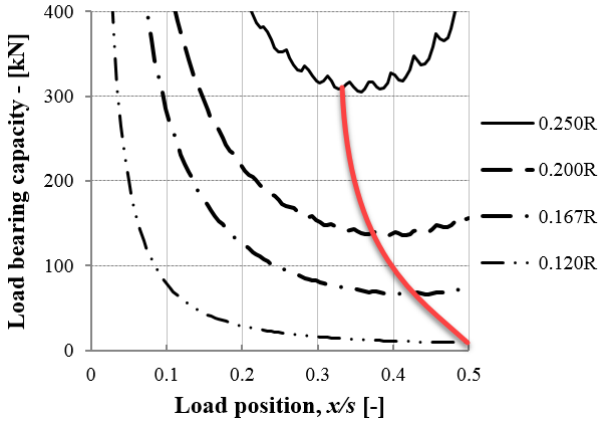

Figure ~~8~~11. Load bearing capacity against the load position in an arch with varying amount of barrel thicknesses (0.250×*R* to 0.120×*R*) as obtained from LimitState:RING 3.

For arches having a thickness greater than 0.3431×R and when the load is applied at crown (x/s = 0.50), the load bearing capacity of the arch tends to infinity; assuming that the material is of infinite stiffness and strength. ~~This is explained in **Figure 9** where~~When the load acting along the axis of symmetry, it can always be balanced by the reactions and the contact forces acting in the interior of the contacts, independently of the actual magnitude of the load. When the thickness (t) is greater than 0.3431×R, two straight thrust lines can always be drawn from the two supports in such a way that they are fully contained in the arch. Indeed, as checked with ~~3DEC~~ discrete element software and also with LimitState:RING software, such an arch had an infinite load bearing capacity. However, the assumption that the elements had infinite stiffness and strength was of course unrealistic.

Commented [T6]: Do we need this?

~~4~~5.2.2 Application of external applied load on masonry skew arches

The critical position of the live load for skew masonry arches has been investigated with the help of the ~~3DEC~~ discrete element software. The geometrical and material parameters of the analysed arches are shown in **Table 1** and **Table 2**. Skew arches were constructed as per the three construction methods (false skew arch, helicoidal method, logarithmic method) ~~(see **Figure 5**)~~. The angle of skew and the voussoirs varied as shown in **Table ~~3~~4**. As mentioned in Section 45.1, it was not possible to use exactly the same voussoir L/W ratios for the three different types of construction of skew arches. Although most of the arches were constructed with voussoirs having L/W ratio equal to 3, in a few cases smaller values had to be applied, remembering that shorter elements reduce the load bearing capacity of the arch, as highlighted in Section 45.1.

Table ~~3~~4. Length to width ratios of voussoirs for the different construction methods of skew arches

	False skew arch			**Helicoidal method**			**Logarithmic method**		
Skew angle	15°	30°	45°	15°	30°	45°	15°	30°	45°
L/W ratio	3:1	3:1	3:1	2.5:1	2:1	3:1	3.1:1	2.9:1	2.4:1

Figures ~~10~~12 and **~~11~~13** show the load bearing capacity of skew arches with thickness equal to 0.12×R and 0.20×R respectively. All arches had the same contact friction angle and equal to 40°. Arches with angle of skew equal to 0° are "regular" or "square arches" and have been studied for comparison purposes. From **Figure ~~10~~12**, the critical position of live load is at the crown of the arch. This is because the critical barrel thickness of regular arches is very close to the critical barrel thickness of false skew arches and equal to 0.120×R. For arches constructed using the helicoidal and logarithmic method of construction, a barrel thickness equal to 0.12×R is far above the critical barrel thickness of an equivalent in shape regular arch (ref. to Forgács et al., 2017). Also, as the angle of skew increases, the critical

position of the live load is moving away from the mid-span to the abutments of the arch. In addition, the trend of the curves in **Figure ~~11~~ 12** is similar to the one in **Figure ~~10~~13**. From **Figure ~~11~~13**, the critical location of the external applied load is around 0.35 – 0.4 times the span of the arch, moving towards the middle span for arches having higher angles of skew.

Moreover, from **Figures ~~10~~ 12** and **~~11~~13**, the ultimate load bearing capacity of skew arches constructed using the false skew method is shown to be almost equal to the load bearing capacity of the regular arches. The load bearing capacity of masonry skew arches constructed using the helicoidal or logarithmic method is higher than the load bearing capacity of the regular arches, for any position of the load along the arch, and for both barrel thicknesses investigated.

Taking into account the 5-6% or 12% decrease of the load bearing capacity due to the smaller applied *L*/*W* ratio of the voussoirs, **Figure ~~10~~ 12 and ~~11~~ 13** show that the application of helicoidal versus the logarithmic method of construction does not considerably increase or decrease the load bearing capacity. Also, from **Figure ~~10~~ 12 and ~~11~~13**, the critical load position is independent of the angle of skew; i.e. the slight differences are due to difference in geometry of the arch.

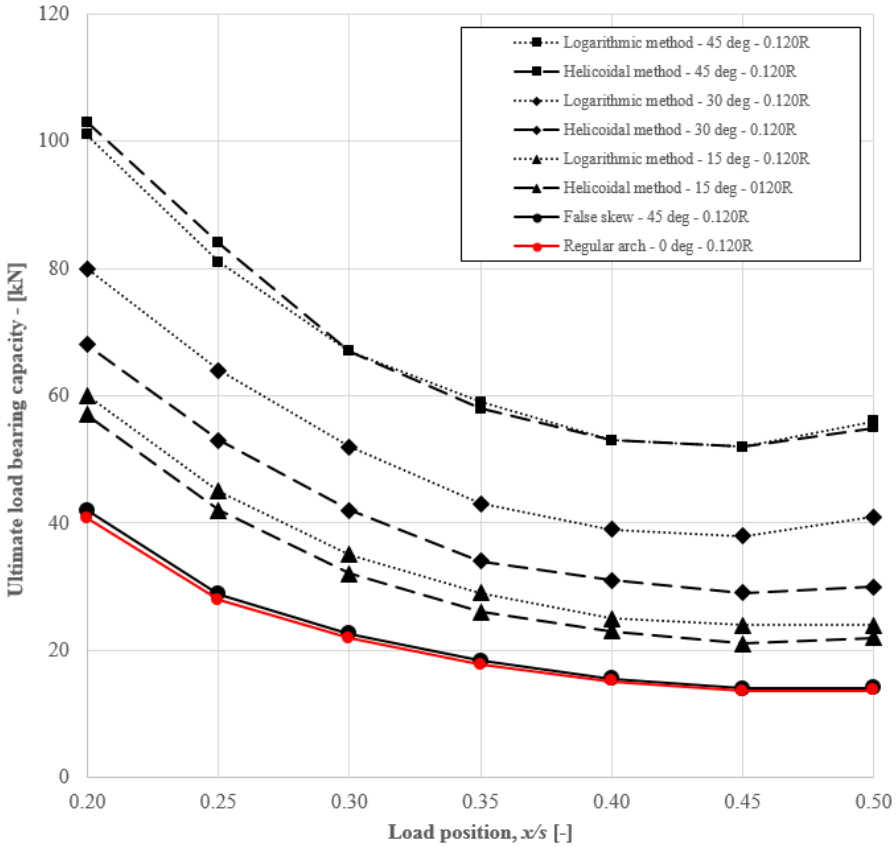

Figure ~~10~~12. Load bearing capacity against load position over span for skew arches constructed using the false skew, the helicoidal and the logarithmic method of construction as obtained from ~~3DEC~~the numerical model. Barrel thickness equal to 0.120×*R*.

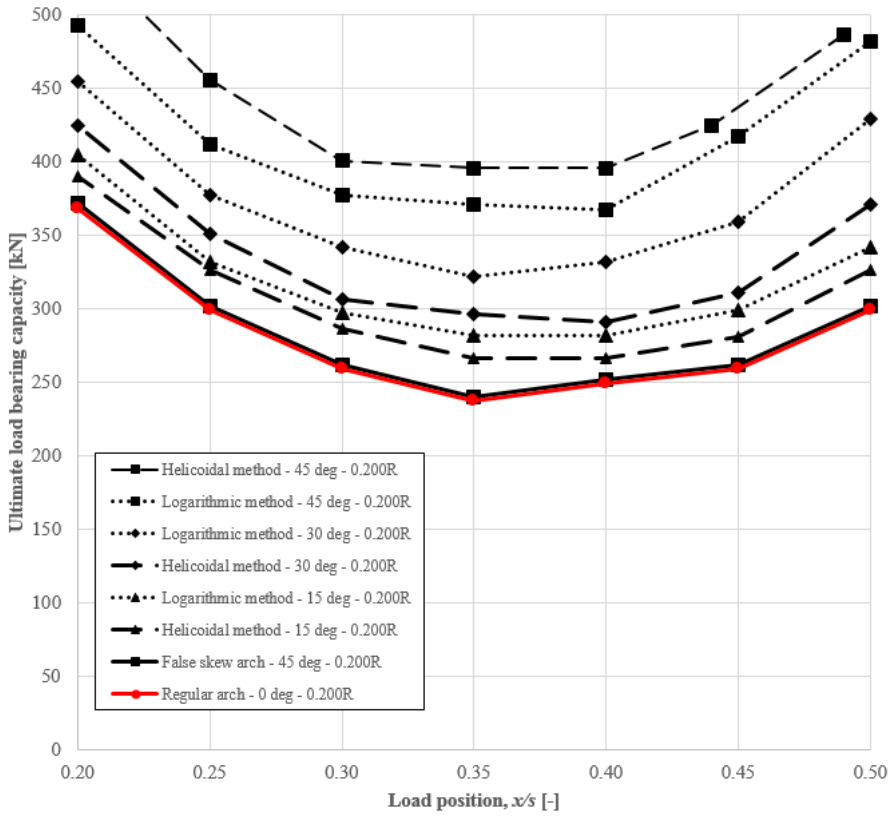

Figure ~~11~~13. Load bearing capacity of skew arches with varying angle of skew (15°, 30°, 45°) and constructed using the: (a) false skew; (b) helicoidal; (c) logarithmic method as obtained from ~~3DEC~~the numerical model. Barrel thickness equal to 0.200 × *R*.

~~**Figure 12** presents the computational results of different in construction 45 degrees skew masonry arches and having barrel thickness equal to 0.20×R. The load bearing capacity (measured on the vertical axis) was plotted against the position of the load and against the contact friction angle (shown on the two horizontal axes). The different colours of 3D plots of surfaces represent different in construction method masonry skew arches. For each construction method, eighty four computational simulations carried out (i.e. every surface is spanned along 84 points). From **Figure 12,** the following comments can be made:~~

Also from **Figures ~~13~~ 14** and **~~14~~15**, the behaviour of masonry skew arches constructed using the helicoidal and logarithmic method is very similar. The masonry skew arches constructed using the helicoidal and logarithmic method also show two different phases of behaviour. In the first phase, the

load bearing capacity of the arch significantly increases with the contact frictional resistance (or friction angle) indicating a sliding-hinging failure mechanism. However, at higher frictional resistance, the slope of the curve in the first phase is lower than the one in the second phase. Section 4.2.3 will show that in the case of larger frictional resistance the failure occurs again according to the four-hinge mechanism, but sliding is necessary to allow the hinges to rotate. In case of $0.120 \times R$ this domain starts at 30° to 32°, while in case of $0.200 \times R$ at 38° to 40°. So the main difference between false skew arch and the logarithmic and helicoidal methods is that during failure the structures utilize the frictional resistance in the course of hinge row development, while in case of false skew arch the neighbouring elements only rotate on each other.

From **Figures ~~13~~ 14** and **~~14~~15,** it is evident that the false skew arch can only reach the load bearing capacity of a regular arch if there is enough frictional resistance between the blocks of the arch. For angle of skew (Ω) equal to 45°, the necessary friction to avoid sliding phenomena is 36°. The minimum necessary frictional angle which can equilibrate the self-weight of the structure in case of masonry skew arches constructed using the helicoidal and logarithmic method is always higher compared to a regular arch, but it is always smaller compared to the false skew method with the same angle of skew.

For arches having barrel thickness (t) *equal to* $0.200 \times R$, the slope of the primary linearly increasing part is the same as the slope of the regular arch, which means that this part does not depend on the angle of skew.

In the realistic range of internal friction (30° - 40°) the structures with the smaller barrel thickness show a significant surplus of the load bearing capacity (+200%) compared to the regular arch, while the surplus in case of the thicker barrel is only +60%. However, if the friction between the blocks in the arch is lower (e.g. 30°, which is perhaps not quite realistic), then the advanced construction methods (helicoidal, logarithmic) show lower load bearing capacity (-30%) than that of the regular arch.

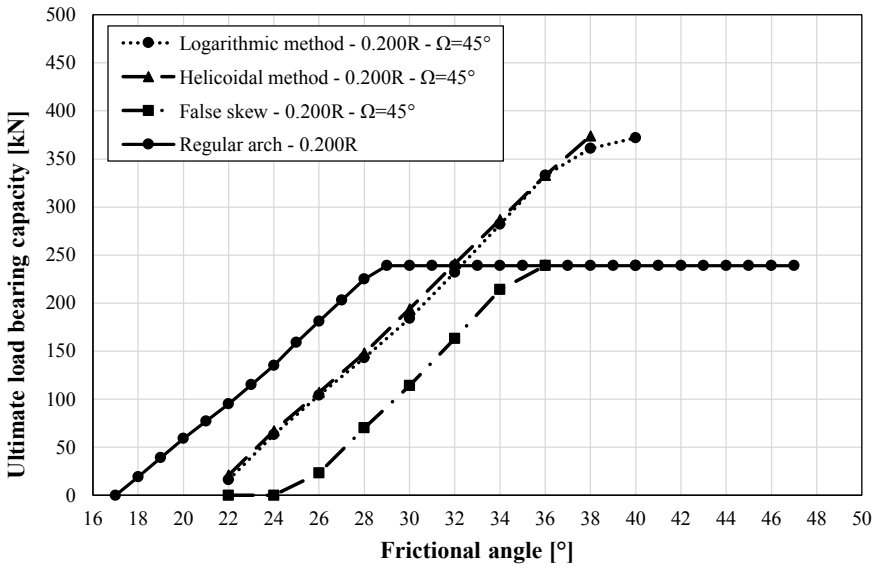

Figure ~~13~~14. Influence of frictional angle on the load bearing capacity (x/s=0.35, b=5.00m, t=0.200×R), Ω=45°

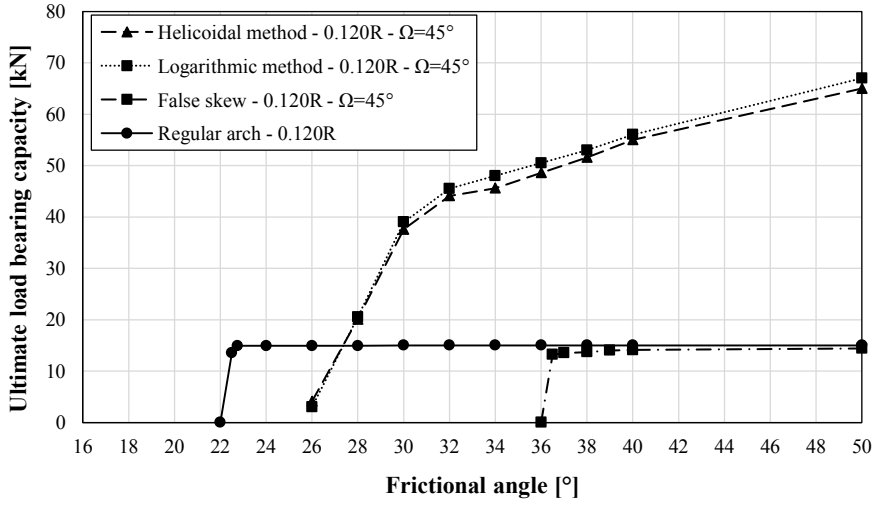

Figure ~~14~~15. Influence of frictional angle on the load bearing capacity (x/s=0.35, b=5.00m, t=0.120×R), Ω=45°

Figure 12~~6~~ ~~presents~~summarises the computational results of different in construction 45 degrees skew masonry arches and having barrel thickness equal to 0.20×R. The load bearing capacity (measured on the vertical axis) was plotted against the position of the load and against the contact friction angle (shown on the two horizontal axes). The different colours of 3D plots of surfaces represent different in construction method masonry skew arches. For each construction method, eighty-four computational simulations carried out (i.e. every surface is spanned along 84 points). From **Figure 12**~~6~~**,** the following comments can be made:

a) When the contact friction angle ranges from 20 to 40 degrees, the load bearing capacity increases linearly with the friction angle. This indicates that frictional sliding takes place during failure.
b) When the friction angle ranges from 40-50 degrees, the load bearing capacity of regular and false skew arches are independent of the frictional resistance. This indicates that the failure mechanism developed is due to hinge development. However, for arches constructed using the helicoidal and logarithmic method, the load bearing capacity is influenced by the contact friction but to a much smaller rate; which demonstrates combination of frictional sliding and hinge development for the formation of the failure mode.

Section 4.2.3 below will reveal the failure modes for different in construction method skew arches. The failure mode significantly influences the load carrying capacity of skew arches and this is captured in **Figure 12**~~6~~.

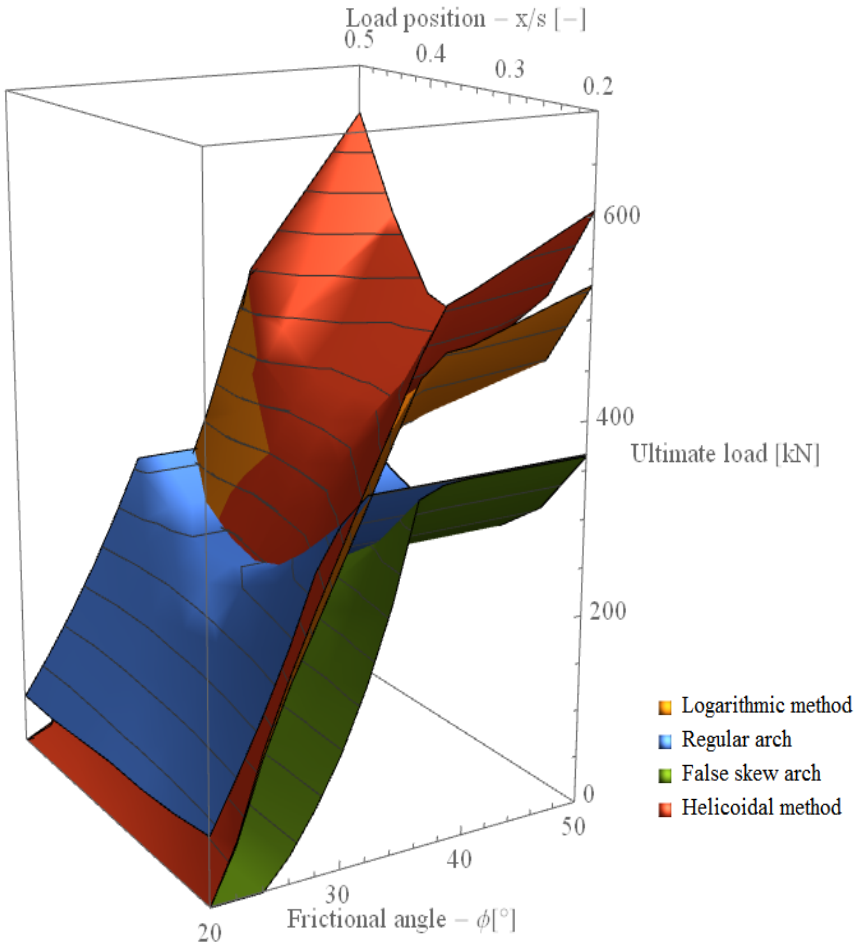
Load position – x/s [–]
0.5
0.4
0.3
0.2
600
400
200
0
Ultimate load [kN]
50
40
30
20
Frictional angle – ϕ[°]
Logarithmic method
Regular arch
False skew arch
Helicoidal method

~~4~~5.2.3 ~~Explanation:~~ Failure modes and contact shear stresses explained

To investigate the failure mechanism of masonry skew arches having different methods of construction, a series of three dimensional models have been constructed. **Figure ~~15~~ 17** shows the failure mode of a false skew arch having thickness equal to 0.200×R and friction angle equal to 40 degrees. From **Figure ~~15a~~17a**, the failure mode of a false skew arch shows a classic four hinge type failure mechanism when the external applied load acts eccentrically to the arch. However, when the external applied load acts in the mid-span, a five hinges failure mechanism observed (**Figure ~~15b~~17b**). However, there may be the case that failure can occur due to pure shear sliding e.g. for a 45 degrees skew masonry arch constructed using the false skew method having low joint frictional resistance equal or less than 30° (**Figure ~~16~~18**).

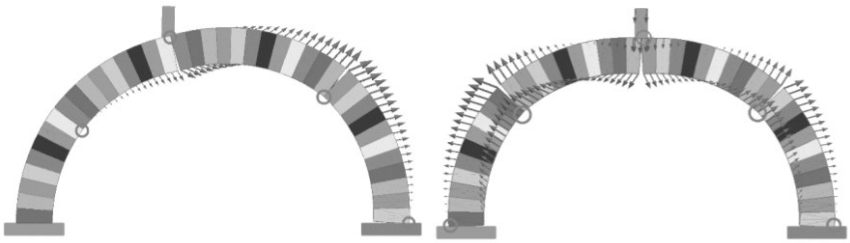

(a) (b)

Figure ~~15~~17. Failure mechanism a false skew arch with barrel thickness equal to 0.200×*R* and friction angle equal to 40°: (a) load applied at quarter-span; and (b) load applied in the mid-span.

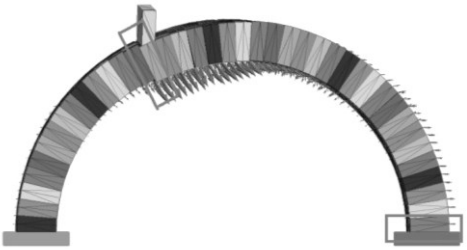

Figure ~~16~~18. Failure mechanism of the false skew arches, in case of 28° frictional degree in the contacts

Figure ~~17~~ 19 compares the failure modes of masonry skew arches constructed using different methods of construction. **Figure ~~17a~~ 19a** shows the failure mechanism of a false skew arch. From **Figure ~~17~~19**, hinges developed parallel to the abutments. This was facilitated by the location of the external applied load, the effect of the stiff abutments and the positioning of the coursing joints. Similar findings

observed by Abdunur (~~1995~~[20]). For skew arches constructed using the helicoidal and logarithmic of construction, hinges developed in a zig-zag pattern and the interface between the blocks at the hinge location does not only open, as in the case of the false skew arch, but also slide upon each other (**Figure ~~17b~~ 19b** and ~~17c~~19c). This additional resistance, caused by the frictional sliding between the adjacent contributes to the overall resistance and load carrying capacity of the arch. Therefore, skew arches constructed using the helicoidal and logarithmic method of construction can carry higher load when compared to skew arches constructed using the false skew method.

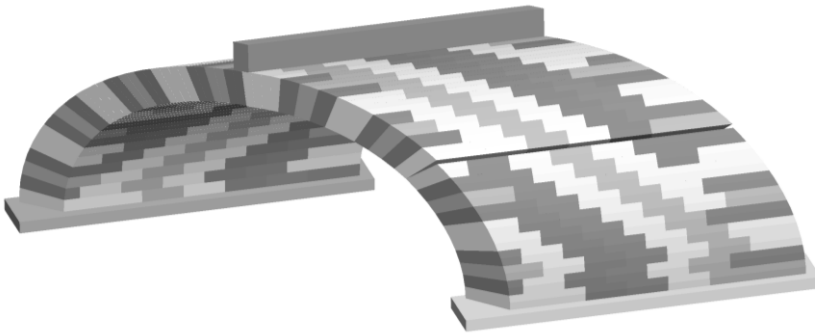

(a) False skew arch

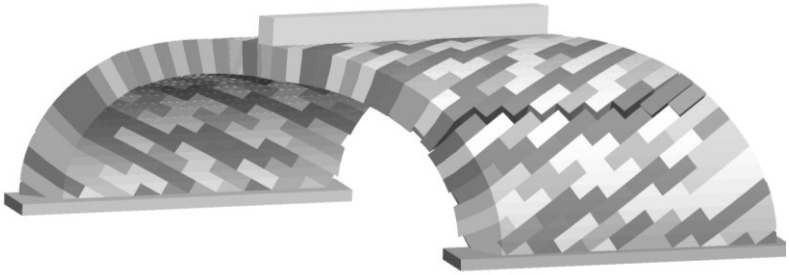

(b) Helicoidal method

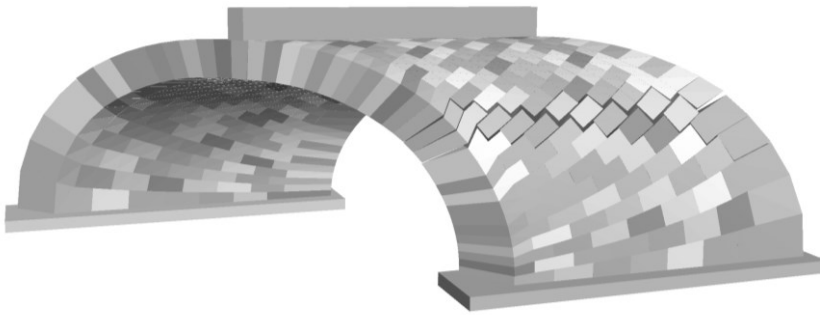

(c) Logarithmic method

Figure ~~17~~19. Failure mechanism for masonry skew arches constructed by the three different methods of construction: (a) false skew; (b) helicoidal; and (c) logarithmic

An investigation has been undertaken to assess the influence of the size of voussoir on the failure mechanism of skew arches. In the case of a false skew arch, a complete different failure mechanism observed for voussoirs having low *L/W* ratios of voussoirs, e.g. L/W<1.25. For arches constructed using short voussoirs (e.g. *L*/*W* equal to 1.0), the face of the skew arch detaches from the internal part of the arch (**Figure** 20~~18~~).

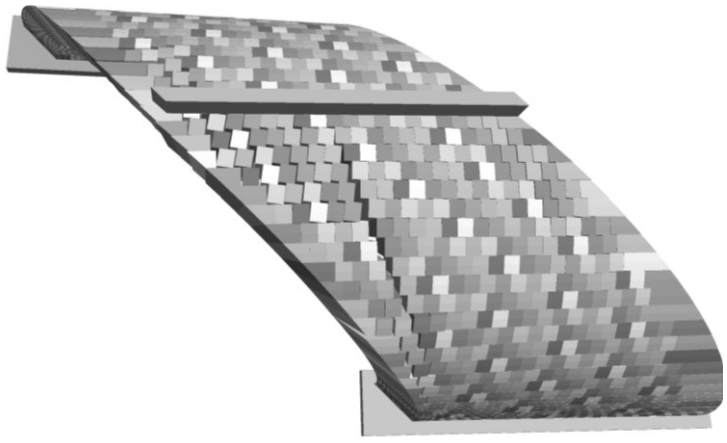

Figure ~~18~~20. Failure mode of false skew arch with *L/W* = 1.0.

Figure ~~19~~ 21 shows the ratio of shear and normal stress for a 45° skew arches ($t = 0.200 \times R$) constructed using the three different construction methods. A full width line load was applied at *x*/*s* equal to 0.35 of

the arch. Deep blue colour denotes areas where the shear stress is zero. Orange and red colours denotes areas where the shear stresses are relatively high compared to the normal stresses. The maximum value of the shear versus normal stress ratio cannot be higher than ~0.84, which value corresponds to 40° frictional angle.

Also the first row in **Figure ~~19~~ 21** shows the ratio of contact shear to normal stress developed in arches due to the their self-weight only (e.g. no live load applied). Under self-weight, in the logarithmic arches the contact forces are mainly perpendicular to the corresponding contact surfaces. However, in the false skew arch at the haunches there are many contacts which are on the verge of sliding.. As the live load increases (second row in **Figure ~~19~~**21), for all the three constructions the shear stresses start to increase particularly in the vicinity of the location of the developing hinges, and stress concentrations also arise at the abutments. At around 240 kN the false skew arch reaches its ultimate load bearing capacity. The arches constructed according to the advance methods can bear further load increments.

From **Figure ~~19~~21**, due to the orientation of the contact surfaces, masonry skew arches constructed using the logarithmic method are least endangered for contact sliding while arches constructed using the false skew method are most exposed to sliding failures when the frictional resistance is low. Also, arches constructed using the helicoidal and logarithmic method, hinging failure occurs in such a way that frictional sliding is mobilized on the contact surfaces at the hinges; this explains the dependence of their load bearing capacity on the frictional resistance.

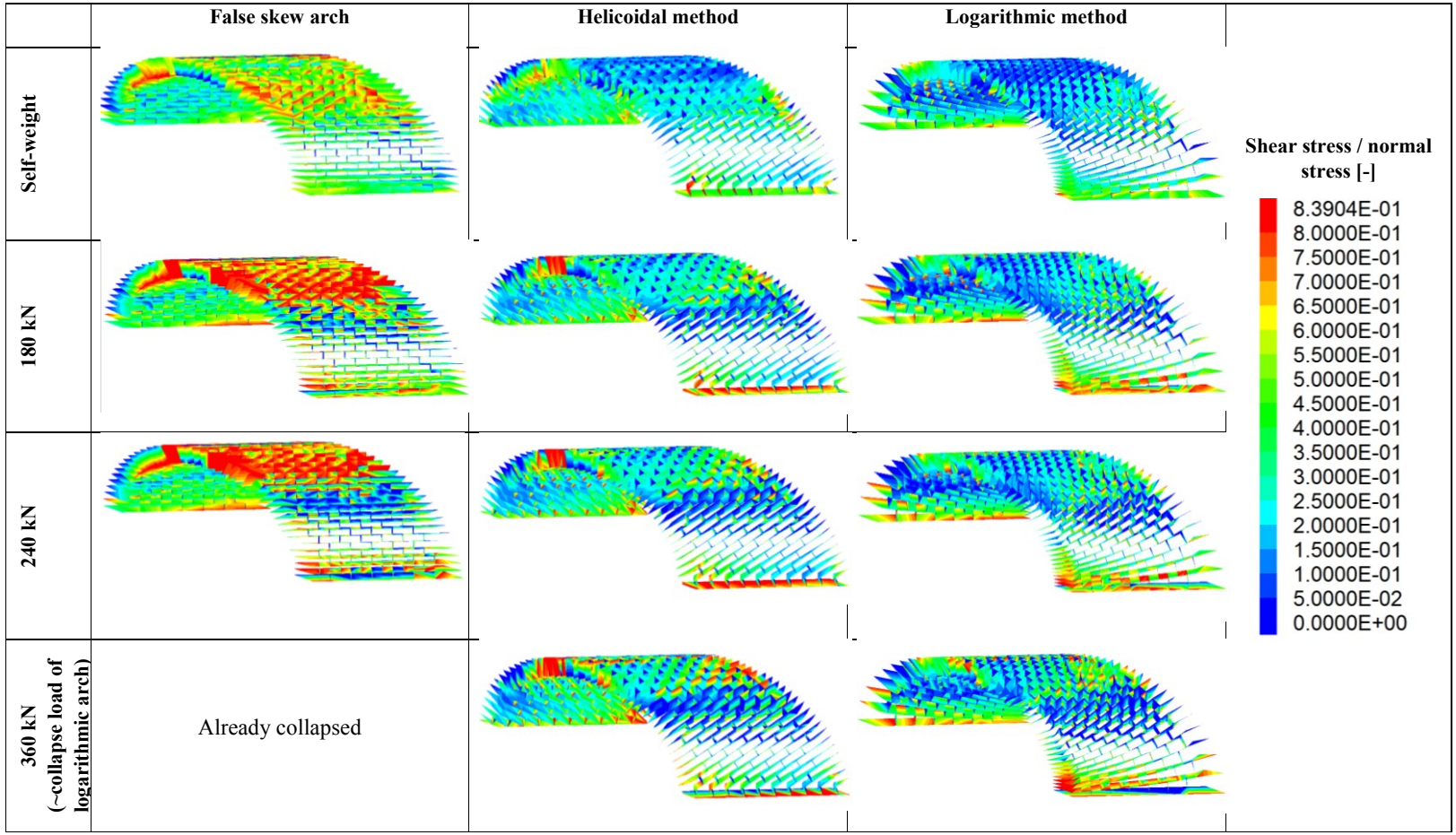

Figure ~~19~~21. Distribution of the ratio of contact shear stress versus normal stress, during the loading procedure until failure

6. ~~5.~~ Conclusions

Formatted: Font: Bold

Formatted: List Paragraph, Numbered + Level: 1 + Numbering Style: 1, 2, 3, … + Start at: 4 + Alignment: Left + Aligned at: 0.63 cm + Indent at: 1.27 cm

In this paper, the influence of construction method (false skew, the helicoidal, and the logarithmic method) on the load carrying capacity of single span, semi-circular skew masonry arches was investigated. Use made of the three-dimensional computational model which is based on the Discrete Element Method. Each stone of the masonry skew arch was represented as a distinct block. Joints were modelled as zero thickness interfaces which can open, close and slide depending on the magnitude and direction of the stresses applied to them. The variables investigated were the construction method, the angle of skew, the width of the arch, the shape of masonry blocks and the location of the load along the span of the arch where the load bearing capacity is minimal. At each skew arch, an increasing full width vertical line load was applied incrementally, until collapse. ~~Numerical results were validated against similar "square" (or regular) arches.~~ From the results analysis, the following conclusions were found:

- For arches whose thickness is close to the critical barrel thickness, the location along the span of the arch where smallest load can be carried (e.g. the critical location) is around the mid-span. Increasing the barrel thickness the critical location gets shifted towards the one-third of the span.
- The critical location of the externally applied load in a masonry skew arch is independent of the angle of skew and the method of construction.
- The ultimate load bearing capacity of skew arches constructed using the false skew method is always less than or equal to the load bearing capacity of the regular arch (i.e. an arch with zero angle of skew) having the same thickness and span. The performance of false skew arches is highly dependent on the frictional resistance of the interface between the voussoirs. False skew arches can have the same load bearing capacity as regular or "square" arches when the internal friction between the elements is high (~40°) and the L/W ratio of the elements is greater than 2.0 (e.g. when the voussoirs are longer in the longitudinal direction).
- In most cases, the load bearing capacity of masonry skew arches constructed using the helicoidal or logarithmic method is higher than the load bearing capacity of regular arches having the same thickness and span. Exceptions can be found in case of unrealistically low frictional angles (i.e. below 32°).
- The behaviour of logarithmic and helicoidal structures was found to be very similar to each other. The small differences between the simulation results can satisfactorily be explained with the slightly different L/W ratios of the voussoirs.
- Three main types of failure mechanisms could be identified for skew arches:
    a) *"Pure" rotational mechanism*: this type of failure can occur in case of high internal friction at the interface of the voussoirs. During failure, four hinge-lines develope in a direction parallel to the abutments. For arches constructed using the helicoidal and

logarithmic method of construction, the hinge formation is always accompanied by sliding of the contact surfaces around the hinges.

b) *Mixed failure*: In case of lower frictional resistances, the failure occurs typically with one sliding and three hinging surface.

c) *Failure of the unsupported acute angled corner*: This failure is typical in case of false skew arch with low L/W ratios of the voussoirs.

- For skew arches constructed using the helicoidal and logarithmic method, hinges developed in a zig-zag pattern and the contacts between the blocks around the hinge location did not only open up as in the case of the false skew arch, but also slide upon each other. This additional resistance, caused by the frictional sliding between the adjacent blocks, contributes to the overall resistance and load carrying capacity of the arch.
- Understanding the mechanical behaviour of skew arches is a difficult task and investigation of different parameters such as geometry, mechanical properties, boundary conditions, etc should be taken into account.

Because of the rigid block assumption, the deformability of voussoirs is neglected and the blocks are prevented against cracking. During previous experimental tests [5, 9, 20] there were no sign of compressive failure. Modelling of bridges with large span might need more realistic assumptions regarding the behaviour of voussoirs.

In the future, additional three dimensional computational models will be developed which will be supported with full scale experimental tests to investigate the influence of rise to span ration, significance of the flexible abutments and the soil and parapet effect on the loading carrying capacity of skew masonry ~~skew~~ arch bridges. ~~Therefore, the influence of the parapets and soil in a masonry skew arch bridge will be investigated.~~

Acknowledgements

The authors express their gratitude to the ITASCA Education Partnership Program ~~for providing a copy of the 3DEC software to assist the above research~~. Also, f~~F~~inancial support of the OTKA 100770 and in Science and Engineering (case/179/65/82) ~~project~~ is gratefully acknowledged.

[1] Brencich A, Morbiducci R. Masonry Arches: Historical Rules and Modern Mechanics. International Journal of Architectural Heritage. 2007;1:165-89.

[2] Sarhosis V, De Santis S, de Felice G. A review of experimental investigations and assessment methods for masonry arch bridges. Structure and Infrastructure Engineering. 2016;12:1439-64.

[3] Forgacs T, Sarhosis V, Bagi K. Minimum thickness of semi-circular skewed masonry arches. Engineering Structures. 2017;140:317-36.

[4] Hodgson JA. The behaviour of skewed masonry arch bridges: University of Salford; 1996.

[5] Wang J. The three dimensional behaviour of masonry arches: University of Salford; 2004.

[6] Heyman J. The stone skeleton. Int J Solids Struct. 1966;2:249-79.

[7] Gilbert M. The behaviour of masonry arch bridges containing defects: University of Manchester; 1993.

[8] Page JJ, Britain) TRLG. Masonry arch bridges: HMSO; 1993.

[9] Melbourne C, Hodgson JA. The behaviour of skewed brickwork arch bridges. Arch Bridges. 1995:309-20.

[10] Pippard AJS, Tranter E, Chitty L. The Mechanics of the Voussoir Arch. Journal of the Institution of Civil Engineers. 1936;4:281-306.

[11] Fanning PJ, Boothby TE. Three-dimensional modelling and full-scale testing of stone arch bridges. Comput Struct. 2001;79:2645-62.

[12] Zhang Y, Macorini L, Izzuddin BA. Mesoscale partitioned analysis of brick-masonry arches. Engineering Structures. 2016;124:142-66.

[13] Zhang YY, Macorini L, Izzuddin BA. Numerical investigation of arches in brick-masonry bridges. Structure and Infrastructure Engineering. 2018;14:14-32.

[14] Milani G, Lourenco PB. 3D non-linear behavior of masonry arch bridges. Comput Struct. 2012;110:133-50.

[15] Vasilis S, Katalin B, José VL, Gabriele M. Computational Modeling of Masonry Structures Using the Discrete Element Method. Hershey, PA, USA: IGI Global; 2016. p. 1-505.

[16] Giamundo V, Sarhosis V, Lignola GP, Sheng Y, Manfredi G. Evaluation of different computational modelling strategies for the analysis of low strength masonry structures. Engineering Structures. 2014;73:160-9.

[17] Cundall PA. A computer model for simulating progressive, large-scale movements in blocky rock systems. Proc Int Symp on Rock Fracture. 1971:11-8.

[18] Lemos JV. Discrete Element Modeling of Masonry Structures. International Journal of Architectural Heritage. 2007;1:190-213.

[19] Sarhosis V, Oliveira DV, Lemos JV, Lourenco PB. The effect of skew angle on the mechanical behaviour of masonry arches. Mech Res Commun. 2014;61:53-9.

[20] Abdunur C. Direct assessment and monitoring of stresses and mechanical properties in masonry arch bridges. Arch Bridges. 1995:327-35.

[21] Hendry AW, Davies SR, Royles R, Ponniah D, Forde MC, Komeyli-Birjandi F. Load test to collapse on a masonry arch bridge at Bargower, Strathclyde. Transport and Road Research Laboratory (TRRL); 1986.

[22] ITASCA. 3DEC - Universal Distinct Element Code Manual. Theory and Background. Mineapolis: Itasca Consulting Group; 2004.

[23] Orbán Z. Assessment, reliability and maintenance of masonry arch railway bridges in Europe. In: P. Roca CM, editor. ARCH 04: 4th International Conference on Arch Bridges. Barcelona, Spain2004. p. 152-61.

[24] Simon J, Bagi K. Discrete Element Analysis of the Minimum Thickness of Oval Masonry Domes. International Journal of Architectural Heritage. 2016;10:457-75.

[25] Sarhosis V, Sheng Y. Identification of material parameters for low bond strength masonry. Engineering Structures. 2014;60:100-10.

[26] Rankine WJM, Millar WJ. A manual of civil engineering1867.

[27] Jiang K, Esaki T. Quantitative evaluation of stability changes in historical stone bridges in Kagoshima, Japan, by weathering. Eng Geol. 2002;63:83-91.

[28] Mosalam K, Glascoe L, Bernier J. Mechanical Properties of Unreinforced Brick Masonry, Section12009.

[29] Sarhosis V, Bagi K, Lemos JV, Milani G, ed. Computational modeling of masonry structures using the discrete element method. USA: IGI Global, 2016.

[30] Kassotakis N, Sarhosis V, Forgács T, Bagi K. Discrete element modelling of multi-ring brickwork masonry arches. In: 13th Canadian Masonry Symposium. 2017, Halifax, Canada: Canada Masonry Design Centre.